Edge Diffusion Flame Stabilization Behind a Step over a Liquid Reactant

Matthew Juniper* and Sébastien Candel†

Ecole Centrale Paris and Centre National de la Recherche Scientifique, 92295 Chatenay-Malabry Cedex, France

The stabilization of a flame behind a step over a liquid reactant is discussed. Dimensional analysis is performed to highlight the parameters that could be influential. Simpler configurations are studied first, including a crossflow flame and the flame in a boundary layer over a liquid fuel without a step. From systematic numerical calculations it is found that the most effective parameter regarding stabilization is the height of the step with respect to the flame's thickness. If the flame is thin, it tucks behind the step and is insensitive to the other parameters. If the flame is thick, it cannot remain in the slow-moving zone behind the step and is exposed to the freestream. It is then very sensitive to the Damköhler number and is readily blown off. The numerical simulations are performed on a configuration that represents a cryogenic coaxial injector between gaseous hydrogen flowing at high speed and a stream of low-speed liquid oxygen. Nevertheless, the non-dimensional results should be valid over a wide range of scales and reactant combinations.

I. Introduction

THE stabilization of nonpremixed flames is often critically important in practical applications. One example is the holding mechanism of the flames in cryogenic rocket engines. In these engines, several hundred coaxial injectors are employed, each with a liquid oxygen core surrounded by an annulus of hydrogen. The flame that forms between the two reactants is stabilized on the lip of the oxygen injector. If it is blown off, the flame can either extinguish entirely or become more susceptible to acoustic feedback. Both of these effects are highly undesirable.

Detailed numerical simulations[1] of this region have been performed using complex chemistry and detailed transport properties at a pressure exceeding the supercritical pressure of oxygen. Although these show that the flame is stabilized behind the liquid oxygen (LOX) tube lip, their high computational cost prevents a parametric study of the factors affecting extinction.

It has recently been shown that the strain rates typically encountered in a rocket motor are insufficient to punch a hole in a diffusion flame sheet formed between hydrogen and LOX.[2] This means that if the edge of this diffusion flame sheet is stabilized behind the lip of the oxygen injector, it cannot be extinguished downstream. The question of stabilization is then reduced to the model problem of a flame edge behind a step over a liquid reactant. It is possible to imagine various arrangements of the streamlines and flame geometry in the near field of the LOX injector. Six possible configurations are represented in Fig. 1. In the first case (Fig. 1a), a recirculation is formed near the step and the flame originates from this region. In the second case (Fig. 1b), the gaseous stream does not separate from the step, mixing takes place between the two reactants, and the flame edge forms farther downstream near the liquid surface. In the third scenario (Fig. 1c), the reactant streams meet at some distance from the surface, and the flame edge appears farther downstream. In Fig. 1d, the gaseous reactant streamline separates from the step while the vaporized reactant streamlines first follow the step before bending in the downstream direction. The flame forms in the near vicinity of the step. Figure 1e shows a situation where vaporization

takes place rapidly, and the liquid vapor velocity is of the order of the gaseous reactant. A crossflow flame is formed around the confluence of the two streams. The sixth geometry, in Fig. 1f, features a double recirculation region and a flame stabilized farther downstream. Systematic calculations carried out in this paper will be used to determine which configuration prevails.

Another objective is to determine the parameters that affect stabilization of the flame behind a step over a liquid fuel. The work, which is theoretical and numerical, clearly shows the flowfield behind the step. The results are compared with experimental data by other authors.[3] Previously it has been assumed that there is a recirculation zone behind the step, of the type found behind bluff bodies. This turns out not to be the case, and a reinterpretation of previous experimental results is necessary.

This study is performed for a simple reaction mechanism that represents hydrogen and oxygen at 1 bar. The choice of a single-step chemistry means that the role of free radicals in the stabilization process cannot be examined. However, the results are expressed in terms of dimensionless parameters, which means that they are valid for all situations that are scale invariant and thermally controlled. The relative influence of these parameters is determined numerically. The result is a criterion that defines stabilization conditions of coaxial jet flames or nonpremixed flames formed behind a splitter plate.

A flame stabilized behind a step over a liquid reactant is a complicated situation. It has features in common with the simpler configurations in Fig. 2, which are a flame in a cross-flow and a flame in a boundary layer over a liquid fuel. It is worth considering these situations and briefly reviewing results obtained via dimensional analysis. This review, carried out in Sec. II, serves to introduce the main characteristic parameters of the problem. This is most successful when applied to simple configurations, where the complete set of variables affecting the system can be listed with confidence.

## II. Review of Some Generic Flame Configurations

A. Crossflow Flame

A simple model problem, recently introduced to the field of combustion[4] is the crossflow flame. This forms between two reactants that approach at 90 deg, perpendicular to the x and the y axes, with identical velocity profiles. One possible geometry is shown in Fig. 2a, where the velocity profiles are linear. Another case of interest features flat velocity profiles. Assume that the mass stoichiometric coefficient s is unity and that the reactants are pure, then a flame head propagates into the premixed region near the origin, trailing a diffusion flame along the line $y = x$. This has many features in common with an edge flame formed between reactant streams that are initially parallel.

*Research Fellow, Laboratoire EM2C, CNRS; currently with Department of Engineering, Cambridge University.

†Professor at Ecole Centrale Paris and Institut Universitaire de France, Laboratoire EM2C, CNRS; candel@em2c.ecp.fr. Member AIAA.
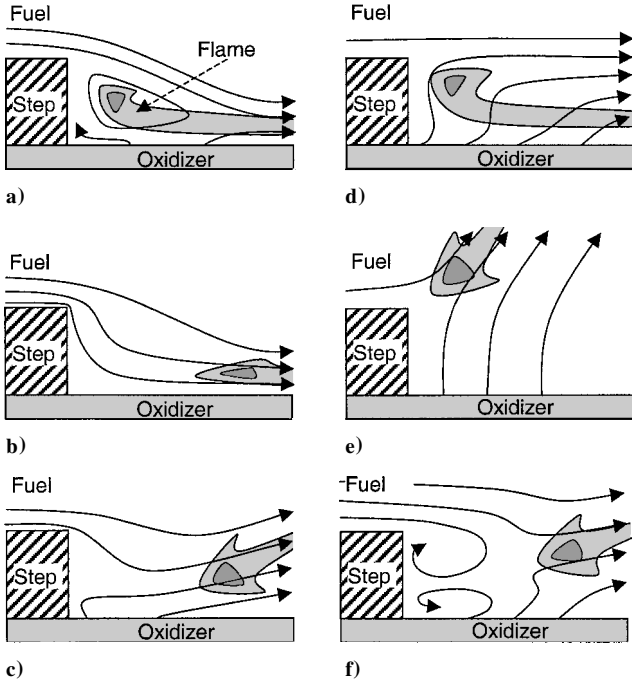
Fig. 1 Various possible flow configurations of a flame behind a step over a liquid fuel: a) gaseous stream separates from step and flame starts in recirculating zone; b) gaseous stream follows step streamline, flame tip is next to liquid reactant; c) both streams meet half-way behind step, where flame forms; d) gaseous stream separates from step, vaporized liquid reactant follows streamline of step, flame forms at top of step; e) liquid reactant vaporizes rapidly, crossflow flame forms above step; and f) double recirculation zone forms behind the step, flame stabilizes downstream.
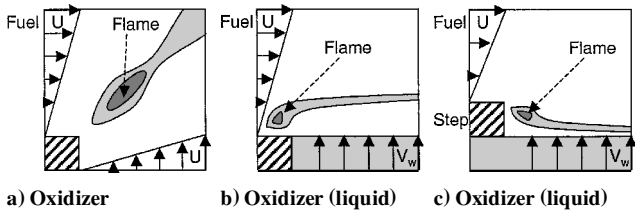
Fig. 2 Flame configurations: a) crossflow flame, in which gaseous reactants impinge perpendicularly with identical velocity profiles, b) flame in a boundary layer over a liquid fuel and c) flame behind a step over a liquid fuel.

Three parameters affect the standoff distance of a crossflow flame.[2] This distance is defined as being from the confluence point of the two streams to the point of maximum heat release. These parameters are a Damköhler number, a Zeldovich number, and a heat release parameter. The last two are constant for any particular fuel. The Damköhler number is defined as $Da_1 \equiv A^{-1/2}\tau_c^{-1/2}$ for a strain rate-controlled crossflow flame, which has inlet profiles $u = Ay$ and $v = Ax$. It is defined as $Da_2 \equiv \mathcal{D}^{1/2}U^{-1}\tau_c^{-1/2}$ for a convection-controlled crossflow flame, which has flat inlet velocity profiles of velocity U. In the previous expression $\mathcal{D}$ is the species diffusivity, which also models thermal diffusivity and viscosity if the Lewis and Schmidt numbers are taken to be unity. The chemical time τ_c can be taken to scale with the ignition time of a homogenous mixture.

In the simple configuration of a crossflow flame, the number of dimensionless parameters is small, and the relationship between them may be discovered by experiments or deduced from systematic calculations. The numerical approach is particularly suitable because a large set of calculations can be performed over a wide range of operating conditions and with small increments in the variables. This tends to the ideal method of performing dimensional analysis, proposed by Weller.[5] The only constraint is the speed of the numerical code, which must enable large numbers of simulations to be performed in a reasonable time span.

This methodology is explained in further detail in Ref. 4. The Navier–Stokes equations are solved with second-order implicit schemes included in the Fluent package. This solution is developed on an unstructured mesh, which can be changed during convergence.

Only the dependence on the Damköhler number is sought because the Zeldovich number and the heat release parameter are constant for a given set of reactants. The non-dimensional standoff distance may be defined as the ratio of this distance L_C to a typical flame thickness $\delta_f \sim (\tau_c \mathcal{D})^{1/2}$. One finds from systematic calculations that the resulting dimensionless group $\Pi \equiv L_c\tau_c^{-1/2}\mathcal{D}^{-1/2}$ is proportional to Da^{-2} for strain rate-controlled and Da^{-3} for convection-controlled flames. In the first case, the standoff distance scales with $L_c \propto A\mathcal{D}^{1/2}\tau_c^{1/2}$, which features a linear dependence with respect to strain rate. In the second case the standoff distance scales with $L_c \propto U^3\tau_c^2\mathcal{D}^{-1}$, which indicates a cubic dependence on the injection velocity U. This process and the results are explained in full detail elsewhere.[2]

B. Flame Above a Porous Plate

Crossflow flames can be formed when one reactant is blown through a porous plate into a perpendicular stream of another reactant. Basic experimental data are available for this situation.[3,6] A further degree of freedom is introduced because the injection velocity V_w may differ from the freestream velocity U. This introduces a further nondimensional parameter, which can be taken to be V_w/U. Two extinction mechanisms are observed.

1) If the injection velocity through the porous plate is high, the flame tip is situated upstream of the plate. As U increases, the flame edge moves downstream, in a similar manner to the convection-controlled corner flame. When it is blown downstream of the leading edge of the plate, the flame tip oscillates. This is because the flame propagates rapidly into the premixed region formed upstream but is blown back when this region contains substantial burnt gases. At higher U, the flame blows off entirely.

2) The second mechanism occurs as the injection velocity through the porous plate decreases. In this case, the flame approaches the plate until it extinguishes through quenching.

It is expected that the first of these mechanisms also occurs over condensed fuel layers. However, the second mechanism could be different because, in the case of a condensed fuel, the injection velocity V_w is a function of the flame position.

C. Flame Above a Liquid Reactant

The situation just described is similar to the flame stationed in a convecting stream above a vaporizing (initially liquid) reactant, a classic problem in combustion theory.[7,8] When the porous plate is replaced by a liquid fuel, no new independent variables are introduced. This is because the velocity of evaporation from the fuel, equivalent to V_w, is coupled to the heat release by

$$V_w = \frac{\lambda}{\rho \Delta h_v}\frac{\partial T}{\partial y} \sim \frac{\lambda}{\rho \Delta h_v}\frac{(T_f - T_s)}{L_{\mathrm{ref}}} \tag{1}$$

where Δh_v is the latent heat of vaporization of the liquid reactant. The increase in temperature between the flame and the surface $(T_f - T_s)$ is given by q/c_p. For the approximate expression to be realistic, L_{ref} must scale with the distance from the surface to the flame. A convenient length scale here, the only one which is independent of the velocity field, is a flame thickness, given by $\delta_f \sim \tau_c^{1/2}\mathcal{D}^{1/2}$. Identifying δ_f with L_{ref} leads to

$$V_w/U = (\lambda/\rho c_p \mathcal{D})\left(\mathcal{D}^{\frac{1}{2}}/U\tau_c^{\frac{1}{2}}\right)(q/\Delta h_v) \equiv Le\, Da(q/\Delta h_v) \tag{2}$$

The first term on the right-hand side is the Lewis number, the second is the Damköhler number, and the third is a nondimensional parameter, which can be used in place of V_w/U. This parameter is equivalent to the Spalding transfer coefficient B_{sp} in the reacting case. [See the definition given subsequently in Eq. (4).] The temperature at the liquid surface is assumed to be uniform in the x direction because it is at, or near to, the boiling point. A temperature gradient

in the x direction would induce a flow in the liquid due to a surface tension difference. However, because of the temperature uniformity, there is no flow here.

In a classical article, Emmons[7] examines the effect of B_{sp}, assuming an infinitely fast reaction rate. A Blasius-like analysis is performed to reduce the Navier–Stokes equations to a simple form. This yields an expression for the vaporization rate (mass per unit time and per unit surface):

$$\dot{m}_v = \frac{1}{2}(\mu_\infty/x)\sqrt{Re_x}\,f(B_{sp}) \tag{3}$$

where B_{sp} is given by

$$B_{sp} \equiv \frac{c_p(T_\infty - T_s) + q_{O2}Y_{O2\infty}}{\Delta h_v} \approx \frac{q_{O2}}{\Delta h_v} \tag{4}$$

The approximate expression on the right-hand side is in the limit when $Y_{O2\infty} = 1$. In this case, the heat released per unit mass of oxygen burned, q_{O2}, far exceeds the enthapy difference in the gas between the freestream and the liquid surface, $c_p(T_\infty - T_s)$.

Numerical calculations[7] for the function $f(B_{sp})$ in Eq. (3) show that the results are well correlated by the following expression:

$$f(B_{sp}) = \frac{\ell n(1 + B_{sp})}{1.7 B_{sp}^{0.18}} \tag{5}$$

An important and not intuitively obvious point is that B_{sp} only has a significant effect on the vaporization rate when $B_{sp} < 10$. With combustion, B_{sp} is of order 100 for most fuels, and consequently, it has little effect. This means, for example, that the latent heat of vaporization has little influence on the burning rate and that the flame cannot quench on the liquid surface. This is because, even if the latent heat of vaporization is very high, the flame moves closer to the surface to increase the vaporization rate. This is confirmed numerically.

The following work has not been reported elsewhere and is of some interest. Its main purpose, however, is to provide background for the discussion of a flame behind a step over a liquid fuel. The numerical formulation used to treat the crossflow flame problem is adapted to study the flame over a condensed surface. The domain is lengthened, to provide room for the flame upstream of the condensed surface. Furthermore, the velocity profile at the bottom boundary is now calculated from the temperature gradient,

$$V_w = \frac{\lambda_s}{\rho_s \Delta h_v} \frac{\partial T}{\partial y}\bigg|_{y=0} \tag{6}$$

The unstructured grid used for this problem is shown in Fig. 3 along with a single solution. The flame head is located upstream from the liquid layer. The flame develops from the edge along a streamline where the reactants meet in stoichiometric proportion. Product and temperature distributions are similar. The oxidizer is located below the flame, whereas the fuel is essentially found above the flame. The latent heat of vaporization Δh_v is initially chosen such that the injection velocity is of the same order of magnitude as for the crossflow flame. This solution acts as a base from which further calculations are made.

The velocity and temperature profiles in a boundary-layer flame above a condensed hydrocarbon have been measured experimentally.[9] The results found in the current analysis are qualitatively similar, as can be seen in Figs. 4 and 5. A quantitative match between calculations and experiments was not attempted because it would have required an excessively large computational domain. This can be seen by noting that the transverse dimension of the domain scales like $U^{1/2}$. It is then interesting to use higher velocities and at the same time reduce the chemical time τ_c to diminish the axial length scale. Axial and transverse length scales are, therefore, not comparable but the general shapes of velocity and temperature profiles are comparable. It is difficult to define reference lengths for the two situations so they are left in dimensional terms. The vaporization profile of the simulations is compared in Fig. 6a with

that predicted by Eq. (3), which is proportional to $x^{-1/2}$. The small jumps in the simulation's profile arise from changes in the grid size around these points, which alters the apparent thermal diffusivity and, hence, the vaporization rate. The agreement is quite good. In Fig. 6b, V_w/U is plotted as a function of B_{sp} at a point 0.5 mm downstream from the flame tip. This shows that V_w does not vary greatly when B_{sp} is above approximately 10, which is the case in any situation involving combustion. Systematic calculations also show that the vaporization rate increases in proportion to $\mathcal{D}^{1/2}$ and $U^{1/2}$ in accordance with Eq. (3).

In the case of the crossflow flame, it was easy to define and measure the flame stand-off distance from the numerical simulations. For the flame above a condensed phase, this is harder because both the x position and the y position of the flame head change. One possibility is to measure the distance along the line of stoichiometric mixture fraction. Two nondimensional parameters may affect this standoff distance: B_{sp} and Damköhler number Da. The flame head lies upstream of the liquid fuel. Its location could only be influenced by B_{sp} if B_{sp} altered the vaporization rate, which does not occur. Consequently, the Damköhler number is the only parameter likely to affect flame stability.
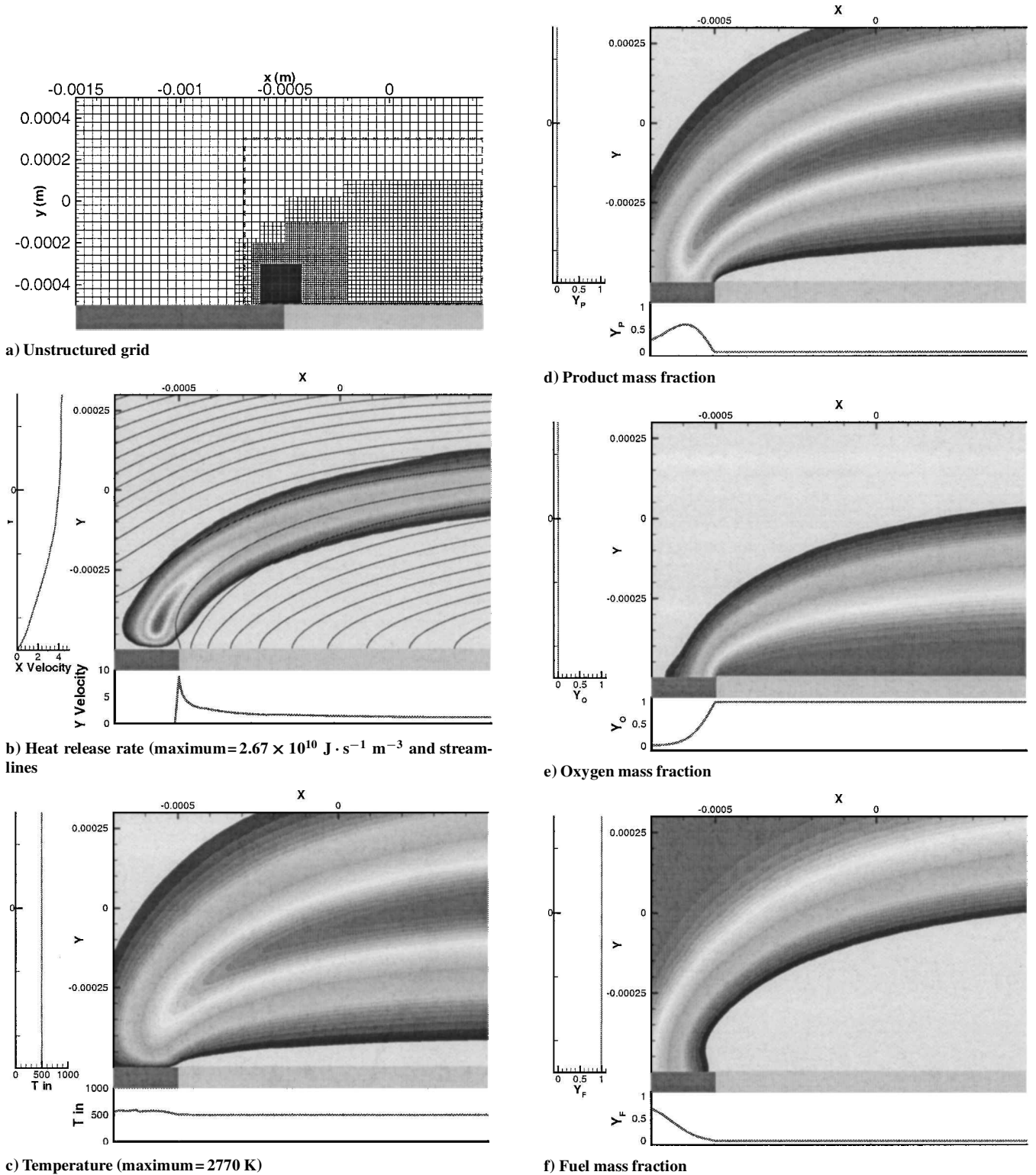
A selection of flowfields near the flame tip is presented in Fig. 7 for various flow conditions. These demonstrate the same behavior as that observed experimentally. When the flame head is upstream of the liquid fuel, numerical convergence is achieved and yields a stationary solution. However, when the Damköhler number based on the freestream velocity decreases, the head of the flame is pushed downstream of the edge of the liquid reactant. When this happens, convergence to a steady state can no longer be achieved, and the flame gradually exits the domain. This probably corresponds to the oscillations found experimentally, although this was not verified with a time-dependent numerical calculation.

III. Stabilization Behind a Backwards-Facing Step

The addition of a backwards-facing step just upstream of the liquid reactant changes the behavior qualitatively.[3] This is already apparent in studies of the gaseous diffusion flame behind a thick splitter plate.[10] The step height h_s is introduced, requiring a further nondimensional parameter. The reference length in this situation is the flame thickness $\delta_f \sim \tau_c^{1/2}\mathcal{D}^{1/2}$. The new dimensionless group is, therefore, $\Psi = h_s \tau_c^{-1/2}\mathcal{D}^{-1/2}$.

Numerical simulations and experiments have been performed[10] on the flame formed behind a splitter plate between nonpremixed gaseous hydrogen and gaseous oxygen flows. The initial stream velocities and densities are U_{H_2}, U_{O_2}, ρ_{H_2} and ρ_{O_2}, respectively and the velocity profiles are essentially flat. When the momentum flux ratio $J \equiv \rho_{H_2}U_{H_2}^2/\rho_{O_2}U_{O_2}^2$ of the two flows is unity, a double recirculation zone is found that is characteristic of the wake behind a bluff body. However, this is the exception rather than the rule. There is usually no recirculation zone behind the splitter plate. Even a small departure of J from unity leads to a situation where the flow with high-momentum flux separates at the corner of the splitter plate, and the flow with low-momentum flux follows the curvature of the plate. The diffusion flame is situated toward the flow with high-momentum flux because the reactants first meet on that side. Despite the fact that there is no recirculation zone, the plate thickness is crucial. It gives the fluid with low-momentum flux some time to heat up, and it ensures that the flame edge remains in a region of relatively low velocity, which aids stabilization. When the thickness of the plate tends to zero, the reactants require a great deal of preheating for flame attachment to occur.[10]

The flow over a porous plate behind a backwards-facing step has been studied experimentally.[3] It is indicated in the preceding section that with no step the flame edge is situated just upstream of the edge of the porous plate, or oscillates just downstream of this edge, or is blown out completely. With the backwards-facing step upstream of the porous plate, two new modes of stabilization appear: lifted and step stabilized. These limit the occurence of oscillations and replace blowout in the range of parameters studied.[3] These are shown in Fig. 8. The plate-stabilized and the oscillating modes can also be

a) Unstructured grid

b) Heat release rate (maximum $= 2.67 \times 10^{10}$ J $\cdot$ s^{-1} m^{-3} and stream-lines

c) Temperature (maximum $= 2770$ K)

d) Product mass fraction

e) Oxygen mass fraction

f) Fuel mass fraction

Fig. 3 Unstructured grid and numerical results for the simulation of a flame over a liquid fuel. Results are shown from the domain outlined by a dashed line on the grid in Fig. 3a: profiles shown below and to the left of each part are taken, respectively, from the bottom and the left boundaries of the entire domain.

observed when the step is not present. In the lifted-flame mode, the flame is positioned halfway between the plate and the top of the step. In the step-stabilized mode, which occurs at higher gas velocities, the flame is stabilized on the lip of the step. As the step increases in size, these modes of stabilization are obtained more readily.

Rohmat et al.[3] interpret these modes of stabilization in terms of a recirculating vortex behind the step, although there is no direct experimental evidence for this. A more likely explanation is that the flows have similar features to the flow behind a gas/gas splitter

plate described at the beginning of this section.[10] At low freestream velocities, the upper flow follows the curvature of the step, leading to a plate-stabilized flame. At high free-stream velocities, the upper flow separates instantly from the edge of the step, leading to a step-stabilized flame. The lifted flame corresponds to a flow somewhat between the two.

Without a step, the parameter B_{sp} has very little influence on a flame above a liquid fuel.[7] However this might no longer apply when there is a step because the boundary-layer approximation used
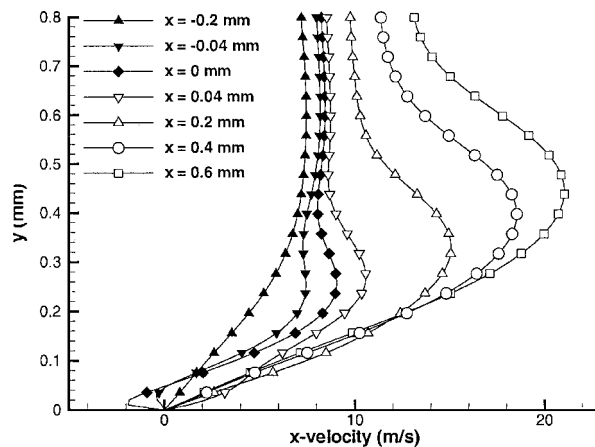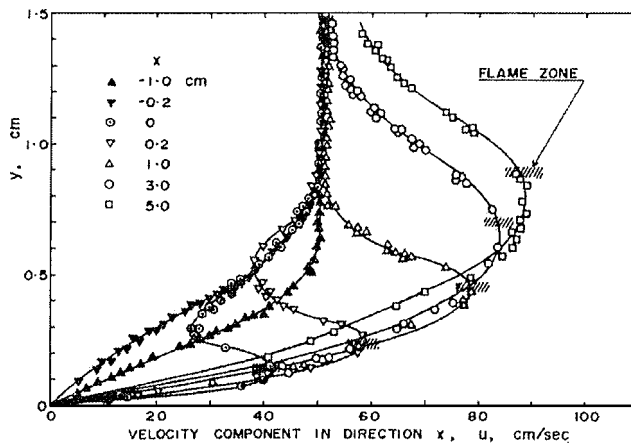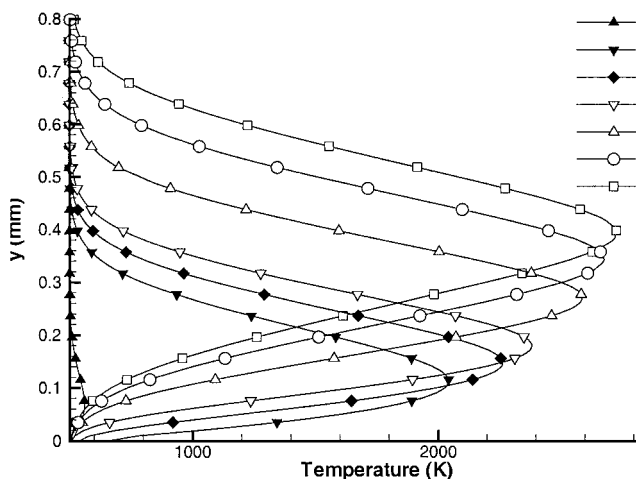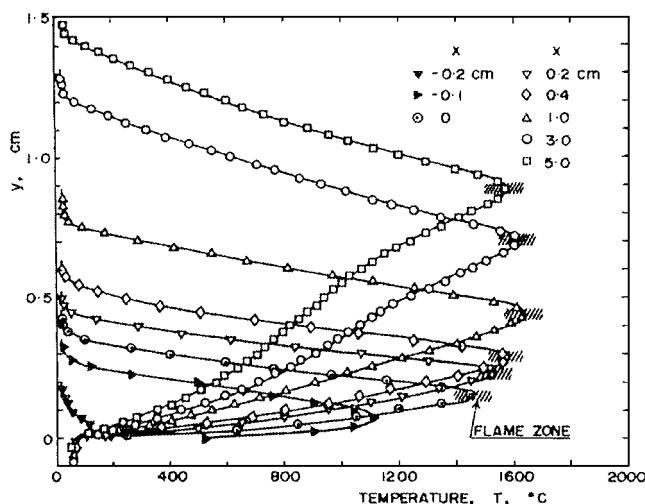
Fig. 4   Qualitatively similiar velocity profiles for a flame above a liquid fuel: a) from a simulation similar to that shown in Fig. 3 and b) from experimental measurements by Hirano and Kinoshita.[9] (Reproduced from Ref. 9 with permission.)

Fig. 5   Qualitatively similiar temperature profiles for a flame above a liquid fuel: a) from a simulation similar to that shown in Fig. 3 and b) from experimental measurements by Hirano and Kinoshita.[9] (Reproduced from Ref. 9 with permission.)

in Emmons's analysis[7] is no longer valid. One then has to consider the effect of three dimensionless groups: Damkohler number Da, B_{sp}, and Ψ. Finally, note that the geometry in Ref. 3 features a distance b between the step and the fuel, whereas in the following analysis the liquid reactant surface begins immediately at the step. Thus, some of the stabilization modes in Fig. 8 will be irrelevant in the following study. The distance b between the step and the fuel is not included in the present study because it does not appear in the injection configuration that motivates this analysis.

A.   Numerical Approach

Numerical simulation is used to pursue the analysis because the problem is not easily described by theoretical means. This relies on a second-order flow solver included in Fluent, combined with the simple reaction and transport scheme reviewed below. The Reynolds number (based on the freestream hydrogen velocity, the lip height, and gas properties in the hot region behind the lip) is around 10^3. This is typical of that characterizing rocket motor injectors. This means that laminar transport can be assumed without the introduction of turbulence models. Transport properties are assumed to vary with temperature as indicated in Table 1. Evaporation from the liquid is modeled, but the interface itself is assumed to be aerodynamically undisturbed by the gaseous stream in this region. According to the results of Oefelein,[11] this is a valid approximation. Steady-state solutions are sought, but some unsteady simulations are also carried out when there is no steady flow solution.

The practical problem that motivates this study involves reaction between oxygen and hydrogen. A simple reaction and transport scheme must be developed to reduce the overall calculation time. A perfect match cannot be obtained between simple and complex reaction/transport models and so it is necessary to match certain factors by assuming a flame-holding mechanism. Experimental results[12] indicate that the flame is stabilized in a slow-moving zone behind the lip of the oxygen injector. Consequently a balance between a residence time and an ignition time seems pertinent. However, it is important to ensure that the premixed laminar flame speed is not considerably different from the true value. Assume a constant heat capacity, then power law expressions for λ, μ, and $\mathcal{D}$ can be used that give constant Lewis, Schmidt, and Prandtl numbers. Given an activation energy,[13] one obtains the following result by approximately matching the heat release, ignition time, and adiabatic flame temperature to a H_2/O_2 flame under similar conditions[2]:

$$k = B[H_2][O_2]^{\frac{1}{2}} \exp(-E_a/RT)$$

with the values given in Table 1. The preexponential factor B is adjusted to obtain the same ignition time as a stoichiometric mixture brought to an initial temperature of 1000 K. Concentrations are in kilomole per cubic meter.

Four values of lip thickness are studied, from 0.2 to 0.4 mm. The meshes are un-structured to permit a high resolution in the influential region just behind the lip. Injection conditions of the

Table 1   Operating conditions for the base cases

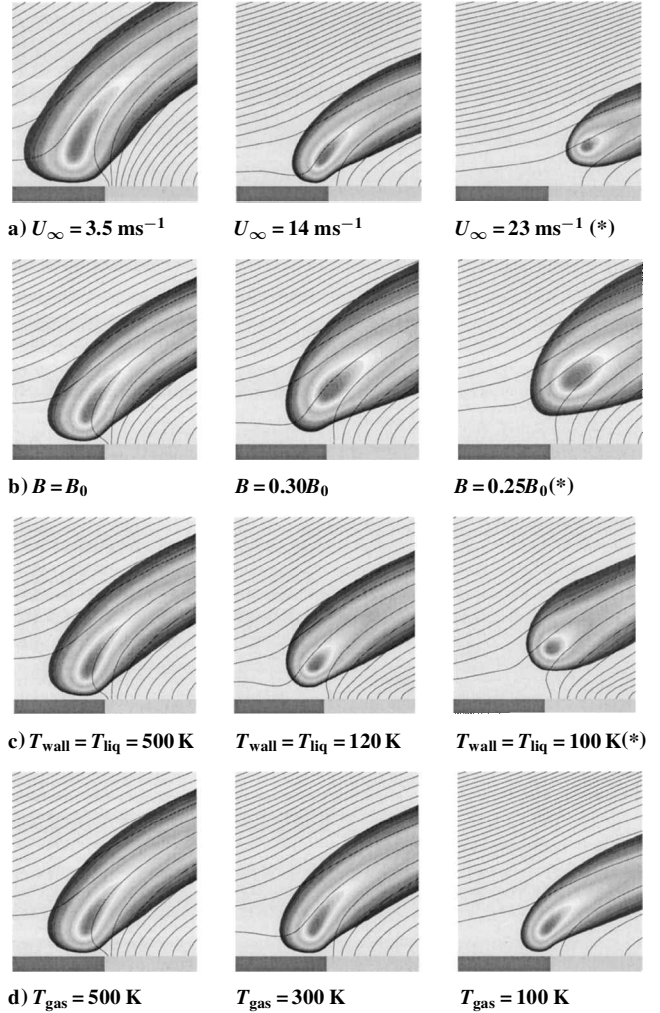| Parameter	Value
Preexponential factor B	2.53×10^9 kmol$^{-1/2} \cdot$ m$^{3/2}$ s^{-1}
Activation energy E_a	9.61×10^7 J $\cdot$ kmol^{-1}
Universal gas constant R	8314 J $\cdot$ kmol$^{-1} \cdot$ K^{-1}
Specific heat capacity c_p	5.35 kJ $\cdot$ kg$^{-1} \cdot$ K^{-1}
Heat release on reaction q	-1.81×10^8 J $\cdot$ kmol^{-1}
Diffusivity $\mathcal{D}$	$2.41 \times 10^{-9} T^{1.76} \cdot$ m^{2}s^{-1}
Conductivity λ	$8.26 \times 10^{-4} T^{0.76} \cdot$ Wm$^{-1} \cdot$ K^{-1}
Viscosity μ	$1.55 \times 10^7 T^{0.76} \cdot$ N $\cdot$ s $\cdot$ m^{-2}
Lip height h_s	0.2–0.4 mm
Temperature of H$_2$ and lip T_{H_2}, T_{lip}	350 K
Hydrogen velocity U_{H_2}	150 ms^{-1}
LOX temperature T_{LOX}	90 K
LOX velocity U_{LOX}	2 ms^{-1}
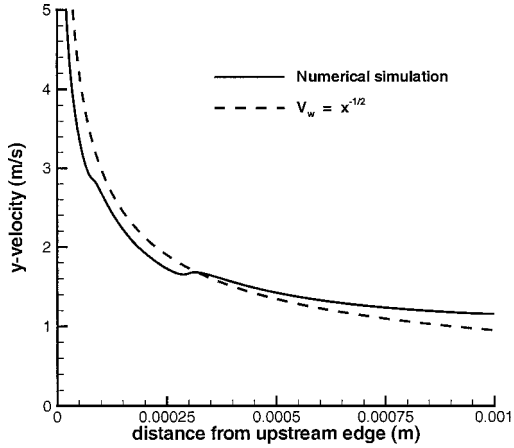
Fig. 6a   Liquid vaporization profile.
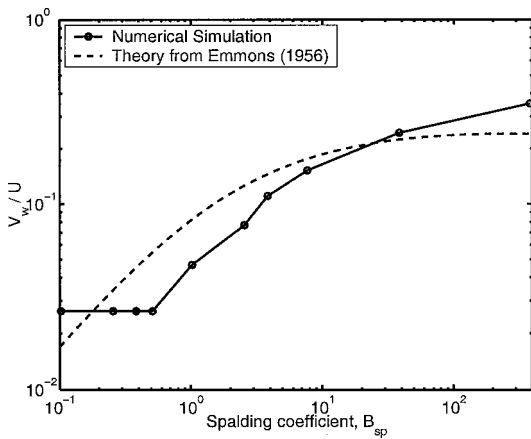
Fig. 6b   Vaporization rate as a function of B_{sp} evaluated from numerical simulations and compared with that predicted by Emmons.[7]

base cases are summarized in Table 1. A typical result is shown in Fig. 9. The flame structure is close to that shown in Fig. 1d. There is no recirculation, the vaporized oxygen reaches the hydrogen stream, and a diffusion flame is formed near the stoichiometric line. The flame edge is close to the step in a region of low velocity. It features a single premixed branch on the gas side of the gaseous reactant. All numerical simulations are carried out at 1 bar. At higher pressures, the flame is thinner and more intense,[1,11] but the general flow structure is that shown schematically in Fig. 1d. The effect of pressure can be encapsulated within the chemical time, which affects both Ψ and the Damköhler number. The results here will be applicable to all situations that are scale invariant with respect to these simulations. We anticipate that this will be the case up to the critical pressure of pure oxygen. Above this pressure the

a) $U_\infty = 3.5$ ms^{-1}   **$U_\infty = 14$ ms^{-1}**   **$U_\infty = 23$ ms^{-1} (*)**

b) $B = B_0$ **$B = 0.30B_0$**   **$B = 0.25B_0$(*)**

c) $T_{\text{wall}} = T_{\text{liq}} = 500$ K   **$T_{\text{wall}} = T_{\text{liq}} = 120$ K**   **$T_{\text{wall}} = T_{\text{liq}} = 100$ K(*)**

d) $T_{\text{gas}} = 500$ K   **$T_{\text{gas}} = 300$ K**   **$T_{\text{gas}} = 100$ K**

Fig. 7   Numerical simulations of a flame above a liquid fuel: shading, heat release rate; ——, streamlines; and (*), unstable solutions.
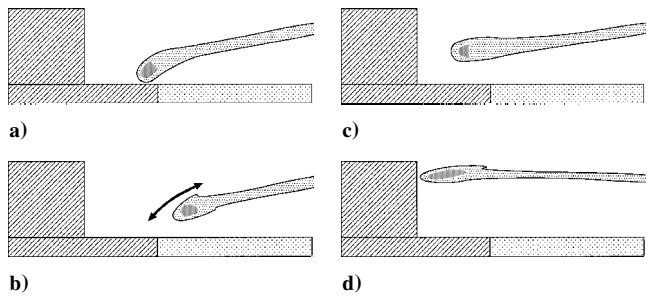

Fig. 8   Position of the flame head behind a step over a liquid fuel or porous plate, from Ref. 3: a) plate-stabilized, b) oscillating, c) Lifted, and d) step stabilized.

physics pertaining to vaporization changes as the gas/liquid interface vanishes, increasing the factor B_{sp}. However, this has no effect on the flame stabilization process and is unlikely to affect the pertinence of Ψ, which is the ratio of the lip thickness to the flame thickness.

B.   Effect of Nondimensional Step Height Ψ

Intuitively, one would expect Ψ to be the most influential parameter. In the limit $\Psi \to 0$, the situation without a step is recovered. The other limit, $\Psi \to \infty$, corresponds to an infinitely thin flame sheet that can readily tuck behind the step. In the first set of simulations, both the flame thickness and the step height are varied to check scale invariance with respect to Ψ. The flame thickness scales with $\tau_c^{1/2} \mathcal{D}^{1/2}$, so that either the chemical time or the diffusivity can be
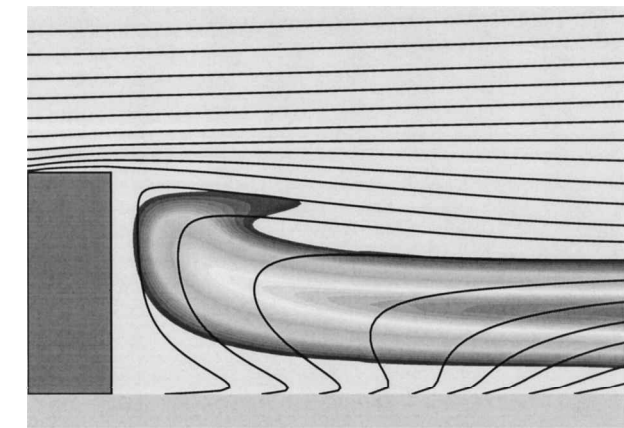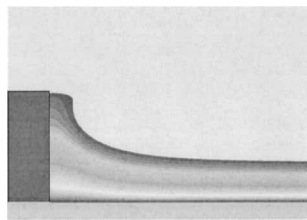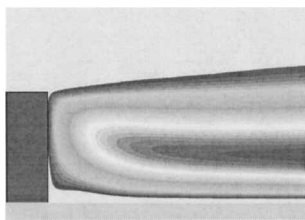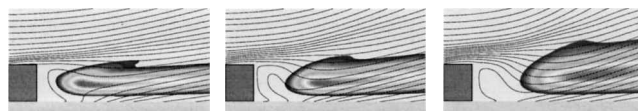
a)
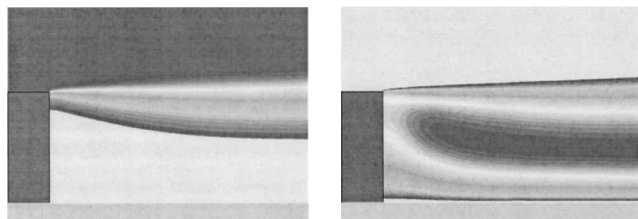
b)
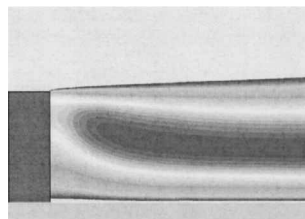
d)

c)

e)

Fig. 9 Hydrogen flame above condensed oxygen tucked behind a step of height 0.4 mm; $U_{H_2} = 190$ ms^{-1}, $T_{H_2} = 350$ K, $T_{LOX} = 90$ K, and $p = 1$ bar: a) streamlines and volumetric heat release (maximum $= 1.2 \times 10^{11}$ J · m^{-3}s^{-1}), b) mass fraction of H$_2$, c) mass fraction of O$_2$, d) mass fraction of H$_2$O, and e) temperature (maximum = 3200 K).


a) $\Psi = 1.25$ b) $\Psi = 1.0$ c) $\Psi = 0.71$

Fig. 10 Flow configurations at different values of ratio of step height h_s to flame thickness δ_f where $U_{H_2} = 150$ ms^{-1} and $T_{H_2} = 350$ K.

changed. This risks changing the Damköhler number because in these simulations, U is held constant: $Da = \mathcal{D}^{1/2}U^{-1}\tau_c^{-1/2}$. $\mathcal{D}$ is increased here because increasing τ_c risks causing extinction via a mechanism involving the Damköhler number.

For each value of h_s, simulations are performed at four values of $\mathcal{D}$. The other molecular transport coefficients, ν and λ, are changed so that the Lewis and Prandtl numbers are unity. Rather than rely on the relation $\delta_f \sim \tau_c^{1/2}\mathcal{D}^{1/2}$, which is only approximate, the flame's thickness across the trailing diffusion flame is measured from the results. It is defined as the distance between the points where the heat release rate is 5% of the maximum.

A sample of the results with $h_s = 0.20$ mm is shown in Fig. 10. In all cases at this high value of U_{H_2}, the hydrogen stream separates from the edge of the step. There are two types of results, depending on Ψ. For $\Psi > 1$, the flame tip is tucked into a slow-moving region behind the step. For $\Psi < 1$, the flame cannot support itself in this region. It becomes exposed to the freestream and blows off. When the step is thick (Fig. 10a), the flame can tuck into the
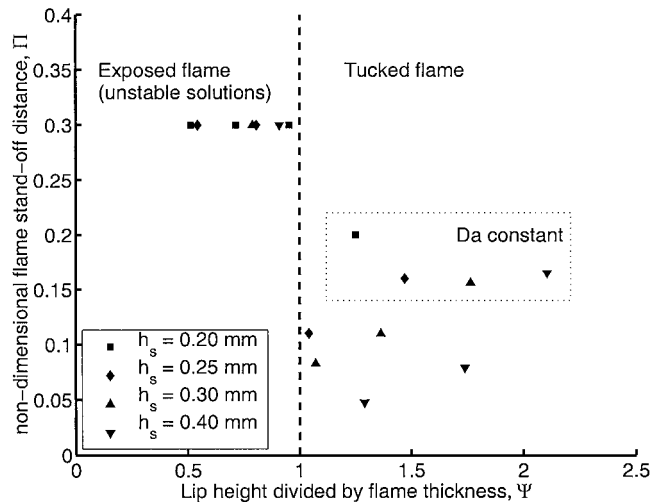
Fig. 11 Flame standoff distance as a function of Ψ for four values of the step height h_s, where $U_{H_2} = 150$ ms^{-1} and $T_{H_2} = 350$ K.

slow-moving region behind the step. The temperatures and mass fractions corresponding to this situation are shown in Fig. 9. This is similar to results in the literature.[10,11] However, when the step is small (Fig. 10c), the flame is forced out of this zone and becomes similar to the situation without a step. It then finds itself exposed to the main stream and is very sensitive to the Damköhler number. When using the steady-state flow solver, the latter type of solution is stable only for low hydrogen velocity (high Damköhler number).

Results from all simulations at all step heights are summarized in Fig. 11. For $\Psi > 1$ the flame stabilizes just behind the step and L_c is measured along the stoichiometric contour. For $\Psi < 1$ the flame is exposed to the main stream. These solutions are unstable and eventually exit the domain. The transition from a "tucked" flame to an unstable "exposed" flame is seen very clearly at $\Psi = 1$. The four simulations in the inset in Fig. 11 are at the same Damköhler number but have different values of h_s. The flame standoff distance is approximately constant, which demonstrates that Ψ has a relatively small effect except around $\Psi = 1$. One can see that, at a given value of h_s, the reduced standoff distance Π diminishes as Ψ is decreased, but this is only because, in these simulations with U constant, the Damköhler number increases when Ψ is reduced.

C. Effect of Spalding Transfer Number B_{sp}

Because $B_{sp} \approx q/\Delta h_v$, either the latent heat of vaporization, Δh_v, or the heat release of reaction, q, can be altered to vary B_{sp}. In these simulations, Δh_v is changed to keep a constant heat release parameter and, hence, a constant adiabatic flame temperature.

With $h_s = 0.4$ mm, B_{sp} is varied over three orders of magnitude. The Stefan flow velocity V_w is measured at a distance of 0.6 mm from the lip, where the profile has become flat. This is plotted as a function of B_{sp} in Fig. 12. The transfer number B_{sp} is approximately 60 in typical cryogenic injectors. It can be seen from Fig. 12 that for such values B_{sp} has some effect on V_w/U. However, increasing V_w has little effect on the flame position and no effect on the flame thickness. Consequently in the range found in cryogenic injectors, B_{sp} does not affect flame stabilization.

D. Effect of Damköhler Number via Changing Hydrogen Velocity

As indicated in Sec. II, a crossflow flame can be described by a convection Damköhler number or a strain-rate Damköhler number, depending on the type of velocity profile in the confluent streams. When the flame is tucked behind a step, it is not clear which Damköhler should be used or on which velocity it should be based. In this section, the effect of the freestream velocity is examined at four step thicknesses: 0.2, 0.25, 0.3, and 0.4 mm. At medium to high U_{H_2}, the tip of the flame remains tucked in a region of slow flow behind the lip, relatively unaffected by the freestream velocity. At very low U_{H_2}, one obtains the flame shape in Fig. 1e.
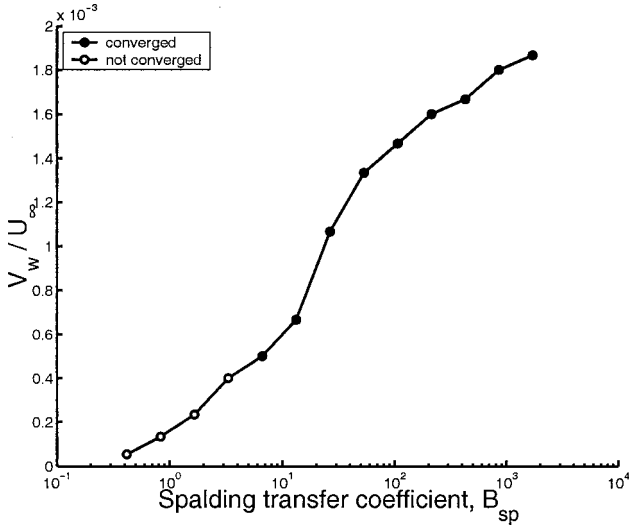
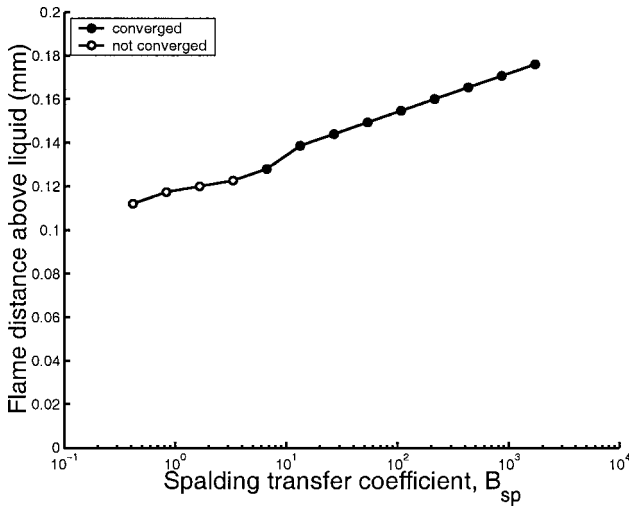**Fig. 12a   Stefan flow velocity.**

Fig. 12b   Distance between liquid and center of trailing diffusion flame as function of B_{sp} for hydrogen flame above condensed oxygen behind a step: step height = 0.4 mm, $U_{H_2} = 150$ ms^{-1}, $T_{H_2} = 350$ K, $T_{LOX} = 90$ K, and $p = 1$ bar.

This effect is quantified for the case where the step height is 0.4 mm. Variables are extracted along the contour of mixture fraction that passes through the center of the flame. (When the flame is close to the liquid core, this is slightly different from the stoichiometric mixture fraction contour.) The flame standoff distance is defined as the position along this contour where the reaction rate passes a certain threshold. This is plotted in Fig. 13a, and the velocity magnitude at this point is plotted in Fig. 13b. Whereas the velocity at the flame edge is proportional to U_{H_2}, the flame stand-off distance is affected very little by U_{H_2}.

When the velocity is increased further, the flow solver does not converge to a stable solution. This is due to aerodynamic instabilities that would lead to vortex shedding off the step in an unsteady simulation. This feature is studied later. It does not affect the main point of this section, which is that flame stability is relatively unaffected by the hydrogen velocity.

E. Effect of Damköhler Number: Varying Hydrogen Temperature

The chemical time in the Damköhler number can be approximated by the ignition time of a homogenous mixture, in which case it depends on T_{H_2}, which is generally the hotter reactant. In the situation behind a step, the flame's thickness becomes a crucial variable. One must ensure that, when one alters the Damköhler number, one does not cause the parameter Ψ to increase above unity, because this induces a qualitative change in the flow. The flame thickness
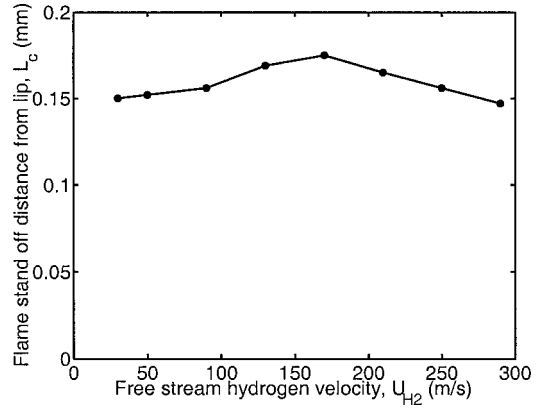

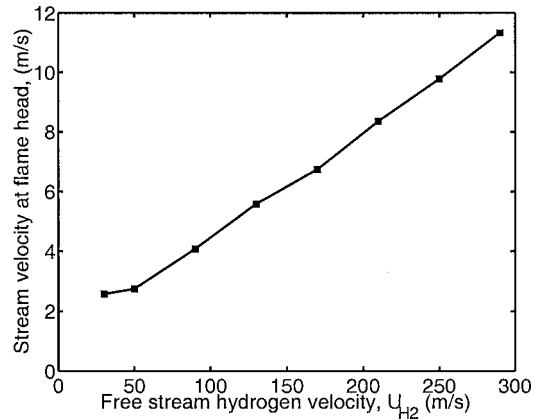**Fig. 13a   Flame standoff distance.**

Fig. 13b   Velocity at flame tip as function of freestream hydrogen velocity: step height = 0.4 mm, $B_{sp} = 60$ ms^{-1}, $T_{H_2} = 350$ K, $T_{LOX} = 90$ K, and $p = 1$ bar.

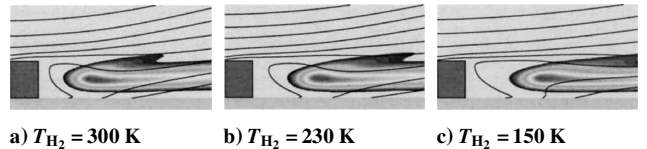a) $T_{H_2} = 300$ K   b) $T_{H_2} = 230$ K   c) $T_{H_2} = 150$ K

Fig. 14   Heat release rate and streamlines for a hydrogen flame above condensed oxygen behind a step; step height = 0.20 mm, $U_{H_2} = 150$ ms^{-1}, $T_{LOX} = 90$ K, and $p = 1$ bar.

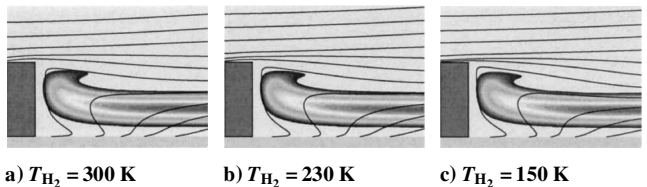a) $T_{H_2} = 300$ K   b) $T_{H_2} = 230$ K   c) $T_{H_2} = 150$ K

Fig. 15   Heat release rate and streamlines for a hydrogen flame above condensed oxygen behind a step; step height = 0.40 mm, $U_{H_2} = 150$ ms^{-1}, $T_{LOX} = 90$ K, and $p = 1$ bar.

scales with $\tau_c^{1/2} \mathcal{D}^{1/2}$. Note that, although this particular chemical time has the usual B^{-1} dependence, it has little dependence on T_{H_2} and should not, therefore, be equated to the ignition time. Consequently, altering the preexponential factor B changes the flame thickness, whereas altering T_{H_2} does not. For this reason, T_{H_2} was altered and B was held constant in the following simulations on step sizes of 0.4 and 0.2 mm. The temperature of the step is held at the freestream temperature.

Results are shown in Figs. 14 and 15 for hydrogen temperatures between 150 and 310 K. When the step is large, the flame position changes very little as T_{H_2} changes, and the flame remains tucked within a region of slow flow. With a smaller step, the

standoff distance increases slightly as the inlet temperature reduces. In both cases, reducing T_{H2} reduces the viscosity, which increases the Reynolds number. Below 150 K, there is no stationary solution, due to aerodynamic instabilities, and the flow solver does not converge to a steady solution. By artificially increasing the viscosity, one can achieve a stable flame once more, even at low inlet temperatures, which suggests that the flame can remain stabilized below 150 K. However, this cannot be taken to be a rigorous demonstration of this proposal.

To study this feature further, two unsteady numerical simulations were performed, one with a step of 0.20 mm and the other with a step of 0.40 mm. The hydrogen inlet temperature was reduced to 130 K for $h_s = 0.20$ mm and to 100 K for $h_s = 0.40$ mm. Frames from these unsteady simulations are shown in Figs. 16 and 17. In the first situation, the flame is almost as thick as the step and, at this low temperature, starts at the downstream end of the slow-moving zone behind the step. Vortices released from the back of the step interact strongly with the flame head, and this eventually leads to extinction.
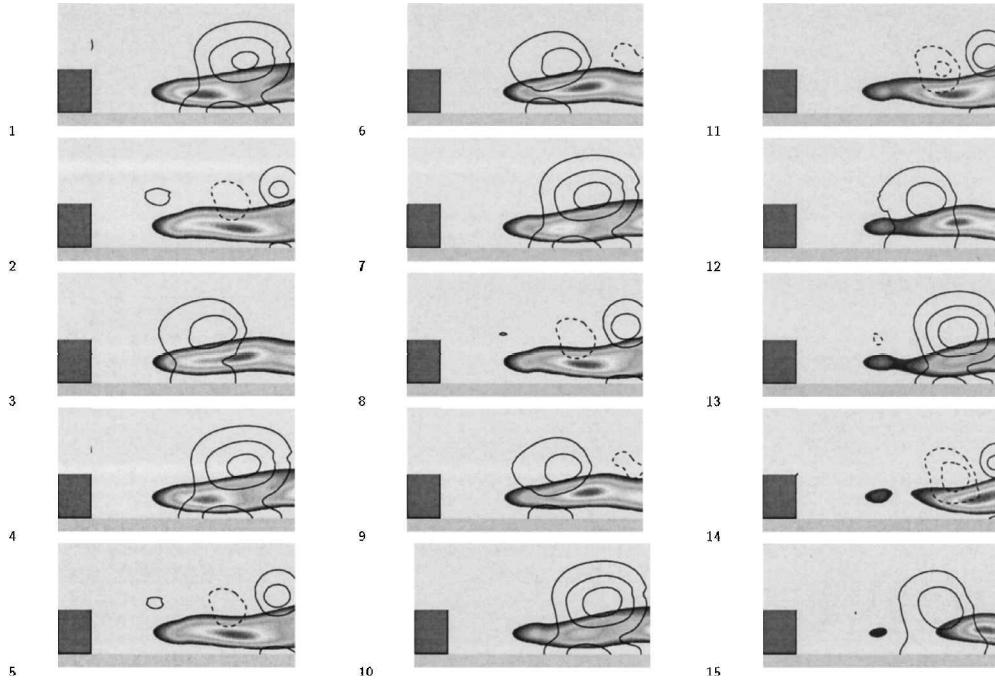
Fig. 16 Heat release rate and pressure contours in an unsteady simulation of a hydrogen flame above a condensed oxygen surface behind a step; step height = 0.20 mm, $U_{H_2} = 150$ ms^{-1}, $T_{H_2} = 130$ K, $T_{LOX} = 90$ K, $p = 1$ bar, and $\Delta t = 0.50$ ms: where – – –, of negative gauge pressure, are vortex cores.
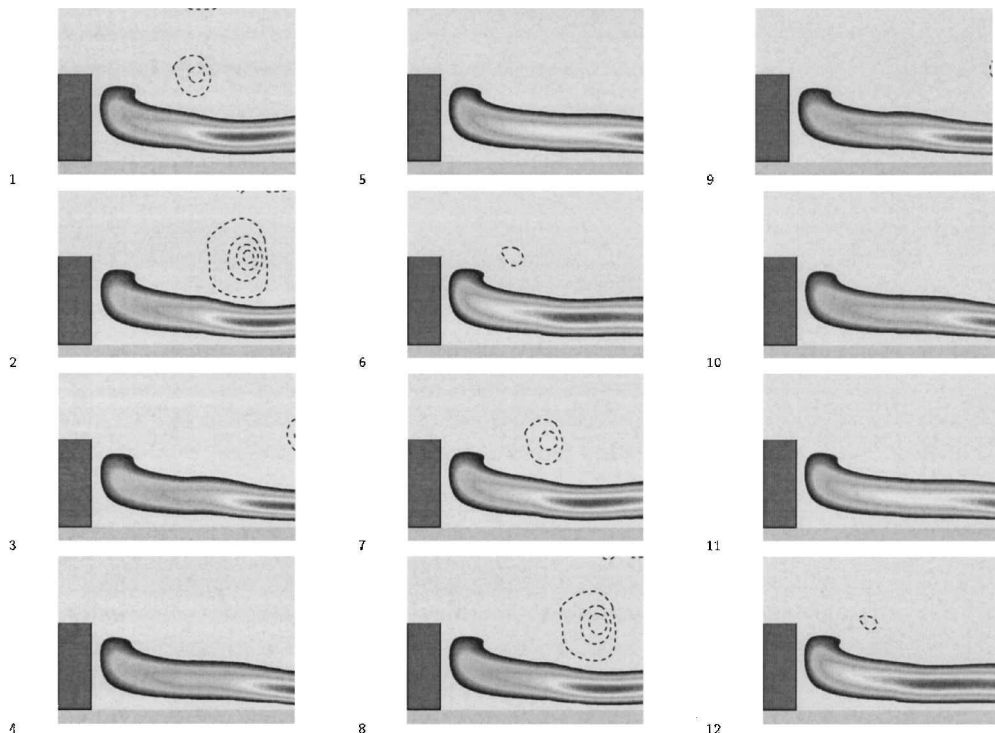
Fig. 17 Heat release rate and pressure contours in an unsteady simulation of a hydrogen flame above a condensed oxygen surface behind a step; step height = 0.40 mm, $U_{H_2} = 150$ ms^{-1}, $T_{H_2} = 100$ K, $T_{LOX} = 90$ K, $p = 1$ bar, and $\Delta t = 0.10$ ms: where – – –, of negative gauge pressure are vortex cores.

In the second situation, the flame is much thinner than the step, and the tip remains well inside the region of slowly moving fluid despite the fact that the step is at a low temperature. The flame is to one side of the line of vortices shed from the step and is unaffected by them. This behavior is seen in a flame to one side of a mixing layer.[14] Vortex shedding has also been described in a detailed numerical study of the stabilization zone of a cryogenic flame,[11] and similarly, the flame is relatively unaffected when situated far from the vortices.

The crucial point here is that if the step is large with respect to the flame thickness, the flame can remain in the region just behind the step, unaffected by vortex shedding, even at low Damköhler numbers. On the other hand, if the step is small, the vortices that are shed interact strongly with the flame tip and can lead to extinction. Consequently, this study of the effect of the Damköhler number highlights once again the importance of the parameter Ψ.

IV. Conclusions

The flame behind a step over a liquid fuel is examined. This configuration is approached systematically, by the use of dimensional analysis to guide a numerical study. Simpler situations, which contain some features common to this flame, are reviewed first. These include a crossflow flame and the flame in a boundary layer over a liquid reactant or porous plate. Three parameters are examined in particular: a Damköhler number, the Spalding transfer number, and the nondimensional step height Ψ. Other parameters that could be influential are the Zeldovich number and the heat release parameter. However, these two are constant for a given set of reactants and, consequently, are not examined here.

The most influential parameter is the nondimensional step height Ψ. When this is large, the flame tucks behind the lip and is affected very little by the Damköhler number. When this is small, the flame is exposed to the freestream and is very sensitive to the Damköhler number or to vortex shedding from the step. In both cases, the Spalding transfer number has little effect on stabilization.

This result can be applied to flames stabilized behind splitter plates or on the lips of coaxial injectors. For reliable stabilization, the plate thickness must be greater than the flame's width.

Acknowledgments

References

[1]Oefelein, J., and Yang, V., "Modeling High-Pressure Mixing and Combustion Processes in Liquid Rocket Engines," *Journal of Propulsion and Power*, Vol. 14, No 5, 1998, pp. 843–857.

[2]Juniper, M., "Structure and Stabilization of Cryogenic Spray Flames," Ph.D. Dissertation, Ecole Centrale Paris, Châtenay-Malabry, France, 2001.

[3]Rohmat, T., Katoh, H., Obara, T., Yoshihashi, T., and Ohyagi, S., "Diffusion Flame Stabilized on a Porous Plate in a Parallel Airstream," *AIAA Journal*, Vol. 36, No. 11, 1998, pp. 1945–1952.

[4]Mahalingam, S., Thévenin, D., Candel, S., and Veynante, D., "Analysis and Numerical Simulation of a Nonpremixed Flame in a Corner," *Combustion and Flame*, Vol. 118, No. 2, 1999, pp. 221–232.

[5]Weller, A., "Similarities in Combustion—A Review," *Selected Combustion Problems*, edited by M. Thring, Vol. 2, Butterworths, London, 1955, pp. 371–383.

[6]Hirano, T., and Kanno, Y., "Aerodynamic and Thermal Structures of the Laminar Boundary Layer Over a Flat Plate with a Diffusion Flame," *Fourteenth Symposium (International) on Combustion*, Combustion Inst., Pittsburgh, PA, 1973, pp. 391–398.

[7]Emmons, H., "The Film Combustion of Liquid Fuel," Zeitschrift für Angewandte Mathematik und Mechanik, Vol. 36, No. 1/2, 1956, pp. 60–71.

[8]Williams, F. A., *Combustion Theory*, Benjamin/Cummings, Menlo Park, 1985.

[9]Hirano, T., and Kinoshita, M., "Gas Velocity and Temperature Profiles of a Diffusion Flame Stabilized in the Stream over Liquid Fuel," *Fifteenth Symposium (International) on Combustion*, Combustion Inst., Pittsburgh, PA, 1975, pp. 379–387.

[10]Deshpande, M., Venkateswaran, S., Foust, M., and Merkle, C., "Finite Splitter Plate Effects on Flame Holding in a Confined Hydrogen–Oxygen Shear Layer," *35th Aerospace Sciences Meeting and Exhibit*, AIAA, Reston, VA, 1997.

[11]Oefelein, J., "Simulation and Analysis of Turbulent Multiphase Combustion Processes at High Pressures," Ph.D. Dissertation, Pennsylvania State Univ., University Park, PA, 1997.

[12]Herding, G., Snyder, R., Scouflaire, P., Rolon, C., and Candel, S., "Flame Stabilization in Cryogenic Propellant Combustion," *Twenty-Sixth Symposium (International) on Combustion*, Combustion Inst., Pittsburgh, PA, 1996, pp. 2041–2047.

[13]Zitoun, R., and Deshaies, B., "Burning Velocities of Rich H_2–O_2 Flames Under Cryogenic Conditions," *Combustion and Flame*, Vol. 109, No. 3, 1997, pp. 427–435.

[14]Delhaye, B., Veynante, D., Candel, S., and Ha Minh, H., "Simulation and Modeling of Reactive Shear Layers," *Theoretical and Computational Fluid Dynamics*, Vol. 6, Nos. 2/3, 1994, pp. 67–87.